Carbohydrate Polymers 93 (2013) 537–546

Contents lists available at SciVerse ScienceDirect

Carbohydrate Polymers

journal homepage: www.elsevier.com/locate/carbpol

Polysaccharide-covered nanoparticles with improved shell stability using click-chemistry strategies

Maxime Laville[a,b], Jérôme Babin[a,b], Isabel Londono[a,b], Mélanie Legros[a,b], Cécile Nouvel[a,b], Alain Durand[a,b], Régis Vanderesse[a,b], Michèle Leonard[a,b], Jean-Luc Six[a,b,*]

[a] Université de Lorraine, Laboratoire de Chimie Physique Macromoléculaire LCPM, UMR 7568, Nancy F-54000, France
[b] CNRS, Laboratoire de Chimie Physique Macromoléculaire LCPM, UMR 7568, Nancy F-54000, France

ARTICLE INFO

Article history:
Received 9 October 2012
Received in revised form
16 November 2012
Accepted 18 November 2012
Available online 22 December 2012

Keywords:
Core/shell nanoparticles
Dextran
Polysaccharide
PLA
Click-chemistry
Colloidal stability

ABSTRACT

Dextran-covered PLA nanoparticles have been formulated by two strategies. On one hand, dextran-g-PLA copolymers have been synthesized by click-chemistry between azide-multifunctionalized dextran ($DexN_3$) and alkyne end-functionalized PLA chains (α-alkyne PLA); then nanoprecipitated without any additional surfactants. On the other hand, $DexN_3$ exhibiting surfactant properties have been emulsified with unfunctionalized or α-alkyne PLA, which are dissolved in organic phase with or without CuBr. Depending on the o/w emulsion/evaporation process experimental conditions, dextran-g-PLA copolymers have been produced *in situ*, by click chemistry at the liquid/liquid interface during the emulsification step. Whatever the process, biodegradable core/shell polymeric nanoparticles have been obtained, then characterized. Colloidal stability of these nanoparticles in the presence of NaCl or SDS has been studied. While the physically adsorbed polysaccharide based shell has been displaced by SDS, the covalently-linked polysaccharide based shell ensures a permanent stability, even in the presence of SDS.

1. Introduction

Nanoparticles, which are defined here as particles with a mean diameter lower than 200 nm, could be used in a wide number of applications. Their submicron size results in a high surface to volume ratio. Consequently, nanoparticles surface characteristics largely control their interactions with surrounding medium, their properties and their potential applications. These characteristics easily be adjusted using specific surfactants in the fabrication process. At the end, these surfactants are physically adsorbed onto the particle core yielding core/shell nanoparticles and the two main characteristics of the covering shell are its density and its thickness.

Among all possibilities, polysaccharide surfactants are very attractive and offer significant advantages. Since the pioneering work of Landoll (Landoll, 1982), such amphiphilic compounds have been prepared by hydrophobic modification of polysaccharides leading to brush-like derivatives. Depending on the hydrophobization degree, these surfactants exhibit emulsifying properties, which can be adjusted. For several years, our previous papers are dealing with polymeric surfactants based on dextran (a neutral bacterial polysaccharide). These surfactants have been produced by chemical modification (Carrier, Covis, Marie, & Durand, 2011; Fournier, Léonard, Le Coq-Léonard, & Dellacherie, 1995; Rotureau, Léonard, Dellacherie, & Durand, 2004; Rouzes, Durand, Léonard, & Dellacherie, 2002) or using polysaccharide derivatives as macroinitiators for several polymerization mechanisms (Dupayage, Save, Dellacherie, Nouvel, & Six, 2008; Nouvel, Dubois, Dellacherie, & Six, 2004; Ouhib et al., 2009).

When drug-delivery applications are considered, the preparation of nanoparticles with polysaccharide based surfaces (Lemarchand, Gref, & Couvreur, 2004) can be carried-out by several processes. Some involve an initial oil-in-water (o/w) emulsion stabilized by a polysaccharidic surfactant (Lemarchand, Couvreur, Besnard, Costantini, & Gref, 2003; Ma et al., 2008; Nouvel, Raynaud, Marie, Dellacherie, Six, & Durand, 2009; Rouzes, Léonard, Durand & Dellacherie, 2003) while amphiphilic polysaccharide can also be nanoprecipitated (Gavory et al., 2011; Jeong et al., 2006; Vila, Sanchez, Tobio, Calvo, & Alonso, 2002; Zhang et al., 2009). Moreover, the polysaccharidic shell can provide biocompatibility, biodegradability and other useful specific properties depending on the targeted application. For instance, hyaluronic acid-covered nanoparticles have been produced for CD44-overexpressing cells adhesion (Jeong et al., 2012; Yadav et al., 2007; Zille et al., 2010), while alginic acid or chitosan shells could be selected for other

* Corresponding author at: Université de Lorraine, Laboratoire de Chimie Physique Macromoléculaire LCPM, UMR 7568, Nancy F-54000, France.
Tel.: +33 03 83 37 52 61; fax: +33 03 83 37 99 77.
E-mail address: Jean-Luc.Six@univ-lorraine.fr (J.-L. Six).

0144-8617/$ – see front matter © 2012 Elsevier Ltd. All rights reserved.
http://dx.doi.org/10.1016/j.carbpol.2012.11.050

specific adhesions (Bravo-OSuna, Vauthier, Farabollini, Palmieri, & Ponchel, 2007; Messai et al., 2005; Wang, Zhou, Sun, & Huang, 2010).

A dextran shell provides colloidal stability because of steric repulsion. But questions related to the surface properties of particles are always relevant for stability considerations as well as for the applications. In previous papers, we showed that hydrophobically modified dextrans could be used as stabilizers to produce stable poly(lactic acid) (PLA) nanoparticles by the o/w emulsion/evaporation technique (Nouvel et al., 2009; Rouzes et al., 2002). Particle analysis studies have shown that the dextran layer was quasi-irreversibly adsorbed onto the particle surface as the brush-like dextran derivatives are multi-anchored. This shell provided protection against non-specific interactions with Bovine Serum Albumin (BSA) and ensured colloidal stability in the presence of salts (Rouzes et al., 2003). Nevertheless, the debate is still open as to the best way to fix dextran-shell on the nanoparticle surface (end-on *versus* side-on coverage) (Bertholon, Vauthier, & Labarre, 2006; Osterberg et al., 1995; Vauthier, Persson, Lindner, & Cabane, 2011).

This paper reports the preparation of PLA nanoparticles covered with a covalently-linked or a physically-adsorbed dextran shell combining o/w emulsion/evaporation or nanoprecipitation process with cupper-catalyzed click-chemistry. Two different synthesis strategies have been designed: (i) $DexN_3$ was reacted by click-chemistry with end-functionalized PLA (α-alkyne PLA) to obtain dextran-g-PLA graft copolymers. Nanoprecipitation of such copolymers produced dextran-covered PLA nanoparticles. (ii) $DexN_3$ was used as stabilizers in the o/w emulsion/evaporation technique with commercial or α-alkyne PLA, in the presence or not of CuBr. The characteristics of nanoparticles in term of size, zeta potential and anchored dextran amount obtained by both strategies are systematically compared. Nanoparticles stability was examined in the presence of salts and dextran-shell anchorage was investigated using an anionic surfactant: sodium dodecyl sulfate (SDS).

2. Materials and methods

2.1. Materials

Dextran T40 [$\overline{M_n} = 34\,000$ g mol^{-1}, Ip = 1.2] was purchased from Sigma-Aldrich and dried under a reduced pressure at 100 °C for one night. No degradation of chains was evidenced under these drying conditions as attested by size exclusion chromatography coupled to a multi-angle laser light scattering detector (SEC-MALLS). 6-Azidohexanoic acid has been obtained from 6-bromohexanoic acid using sodium azide in DMSO at room temperature (Zhang et al., 2010). Carbonyldiimidazole (CDI), propargyl alcohol, dimethylformamide (DMF), PLA [$\overline{M_n} = 35\,000$ g mol^{-1}, Ip = 1.3, inherent viscosity 0.55–0.75 dL/g], stannous octoate ($SnOct_2$), copper bromide (CuBr), sodium dodecyl sulfate (SDS), ethylenediaminetetraacetic acid (EDTA) were purchased from Sigma–Aldrich–Fluka and were used without any further purification. D,L-Lactide from Lancaster was recrystallized twice with dry toluene and dried under vacuum before use. Dimethyl sulfoxide (DMSO) and toluene were refluxed, distilled over CaH_2 and then added in the reaction media *via* cannula under nitrogen atmosphere.

2.2. $DexN_3$-*n*

Compound 1 (Scheme 1) has been obtained by reaction between 6-azidohexanoic acid (12.88 g, 80.5 mmol) and CDI (14.5 g, 88.55 mmol) in 200 mL CH_2Cl_2 during 2 h at room temperature. 6-Azidohexanoic acid has been diluted with CH_2Cl_2, then added dropwise to the CDI solution while CO_2 bubbles have been produced. After the reaction, compound 1 has been recovered by washing, drying and solvent evaporation (88% yield). General synthesis of $DexN_3$-24: dried dextran (2.18 g, 13.4 mmol glucosidic units) has been dissolved in 20 mL DMSO and 0.7 g (3.35 mmol) of compound 1 per 100 glucose units has been added. The reaction has been carried out at 50 °C during 2 days, then azido-functionalized dextran has been recovered by precipitation from ethanol. Depending on experimental conditions, $DexN_3$-*n* has been obtained, where *n* is the modification degree *i.e.* the number of N_3 groups per 100 glucose units. Characteristics of such derivatives have been given in S1 (see supporting info). Modification degree (*n*) has been estimated by ^{1}H NMR in DMSO-d_6 (see supporting info S2) using Eq. (1) where A_f, A_g and A_h are the areas of 6 protons of alkyl chains (from 1.3 to 1.6 ppm). A_a is the area of the anomeric proton centered at 4.7 ppm:

$$n = \frac{(A_f + A_g + A_h)/6}{A_a} \times 100 \quad (1)$$

2.3. α-Alkyne PLA

General synthesis of PLA_{5200}: propargyl alcohol (0.1466 g, 2.61 mmol) and $SnOct_2$ (0.0318 g, 0.0785 mmol) have been dissolved in dry toluene, separately. Each solution has been transferred to a hot D,L-lactide (11.31 g, 78.5 mmol) solution in 54 mL toluene (80 °C), under nitrogen flow. To reduce transesterification side reactions, a $SnOct_2$/OH functions molar ratio equal to 0.03 has been used (Nouvel, Dubois, Dellacherie, & Six, 2004). Consequently, each PLA chains exhibit one alkyne end-function. Polymerization temperature was kept at 100 °C for 16 h, then the polymerization has been stopped by addition of a catalytic amount of acidic methanol. Polymer was precipitated twice into cold ethanol. $\overline{DP_n}$ of each α-alkyne PLA was determined from ^{1}H NMR spectrum of purified product in $CDCl_3$ using $\overline{DP_n} = B/(C/2)$ where *B* and *C* are the areas of PLA methyne protons (5.2 ppm) and of CH_2 protons from initiator group (4.7 ppm), respectively. Peak characteristic of HC≡ proton was observed at 2.5 ppm.

2.4. Dextran-g-PLA produced by click-chemistry

General synthesis of Dex-g-14PLA_{5200}-g-10 N_3: syntheses have been carried out after dissolving $DexN_3$-24 (0.501 g, 0.61 mmol of N_3) and α-alkyne PLA_{5200} (1.93 g, 0.37 mmol of alkyne functions) in DMF (Scheme 1). 1 equiv. of CuBr (87 mg) and 0.1 equiv. of Cu^0 (3.9 mg) per N_3 function have then been added and the reaction was left to proceed under stirring during one day at room temperature. After reaction, the crude medium has been filtered and diluted by acetone/water mixture (95/5, v/v), then precipitated from an EDTA aqueous phase. Extraction of non-grafted PLA chains has been realized by washing with acetone/diethylether (80/20, v/v). The efficiency of this elimination has been proved by ^{1}H NMR in DMSO-d_6 and by SEC (see supporting info S3). Yield of click-chemistry was estimated to be higher than 98%. Depending on experimental conditions, Dex-g-*x*PLA_m-g-*y*N_3 have been obtained, with *x* and *y* the number of PLA grafts ($\overline{M_n}$ equal to *m*) and of residual N_3 groups per 100 glucose units, respectively. When dextran-g-PLA copolymers exhibit no residual N3 functions, their names will be Dex-g-*x*PLA_m. Characteristics of such copolymers have been given in Table 1. *x* was estimated using Eq. (2) where A_a and *T* are the areas of the anomeric proton (4.7 ppm) and of the proton of each triazole ring (8.15 ppm), respectively. *y* was calculated from $(n - x)$ where *n* is the modification degree of $DexN_3$-*n*.

$$x = 100\frac{T}{A_a} \quad (2)$$

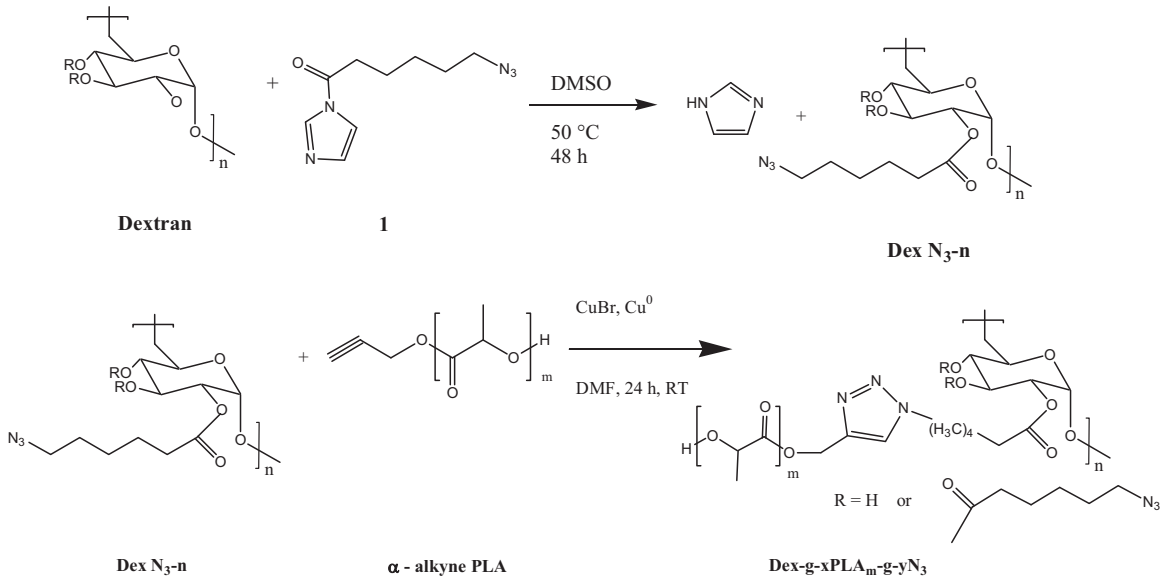

Scheme 1. Syntheses of $DexN_3$ and Dextran-g-PLA.

Table 1
Dex-g-xPLA$_m$-g-yN$_3$ characteristics.

Dex-g-xPLA$_m$-g-yN$_3$	DexN$_3$-n*	α-Alkyne PLA (M_n g/mol)	ρ_{PLA} [a]	Theoretical M_n [b] (g/mol)	dn/dc	SEC M_n [d]	N_{grafts} [c]
Dex-g-9.5PLA$_{8000}$	DexN$_3$-9.5	8000	81	196 300	0.035	152 300	15
Dex-g-14PLA$_{5200}$-g-10N$_3$	DexN$_3$-24	5200	79	198 200	0.029	229 600	36
Dex-g-42PLA$_{1600}$	DexN$_3$-42	1600	75	187 300	0.039	196 500	95
Dex-g-82PLA$_{1000}$	DexN$_3$-82	1000	75	230 000	0.036	184 200	133

[a] From Eq. (3).
[b] From Eq. (4).
[c] From Eq. (5).
[d] For explanations, see Section 2.

Moreover, each copolymer could also be characterized by the PLA weight fraction (ρ_{PLA}) estimated from Eq. (3) where 162 and 301 are the molar masses (g/mol) of glucose unit and glucose unit carrying one N_3-end alkyl chain, respectively.

$$\rho_{PLA} = \frac{x * n * m}{x * n * m + n * 301 + (100 - n) * 162} * 100 \quad (3)$$

Knowing the number of PLA grafts (x), the theoretical $\overline{M_n}$ of dextran-g-PLA has been calculated using Eq. (4), where 139 is the molar mass (g/mol) of the N_3-end alkyl chain. From this theoretical $\overline{M_n}$, the theoretical average number of PLA grafts per copolymer chain (N_{grafts}) was easily estimated from Eq. (5).

$$\text{Theoritical}\,\overline{M}_n = \overline{M}_{n_{\text{dextran}}} + \frac{\overline{M}_{n_{\text{dextran}}}}{162} * n * (m * x + 139) \quad (4)$$

$$N_{grafts} = \frac{\text{Theoritical}\,\overline{M}_n - \overline{M}_{n_{\text{dextran}}}}{m + 139} \quad (5)$$

2.5. Nanoprecipitation of clicked Dex-g-xPLA$_m$-g-yN$_3$

Nanoprecipitations have been performed at ambient temperature by a classic technique (Gavory et al., 2011). 50 mg of Dex-g-xPLA$_m$-g-yN$_3$ have been dissolved in 5 mL of acetone/water (95/5, v/v) for 24 h, then added dropwise to 10 mL of water under magnetic stirring. Complete addition was achieved in 15 min. The suspension has been maintained under magnetic stirring for 10 min, then solvent has been evaporated 2.5 h at 37 °C. The crude suspensions have then been centrifuged for washing (8500 rpm, 75 min at 15 °C). The supernatant containing nanoparticles has been freeze-dried.

2.6. o/w emulsion/evaporation technique

The nanoparticles have been prepared by an o/w emulsion method as follows: 25 mg of either commercial PLA or α-alkyne PLA or a 50/50 blend of both have been dissolved in 1 mL of CH_2Cl_2. 10 ml of an aqueous solution (CH_2Cl_2-saturated) of DexN$_3$-n at 5 mg/mL have been degassed by N_2 bubbling during 30 min. The organic phase has been added under vigorous stirring to the aqueous one. 5 mg of CuBr has been rapidly added to this emulsion and the mixture has then been sonicated (pulsed mode, 10 W, 2 min in an ice bath) using a Vibracell 75043 model (Bioblock Scientific). The solvent has been evaporated at 37 °C for 2.5 h. Finally EDTA has been poured into the resulting suspension and let to stir for one day to complex CuBr. Suspensions have then been centrifuged (8500 rpm, 75 min at 15 °C) and the collected nanoparticles have been re-suspended in water, then centrifuged again in order to remove the non-adsorbed dextran derivatives (Rouzes et al., 2003). The supernatant containing nanoparticles has been freeze-dried. To characterize Dex-g-xPLA$_m$-g-yN$_3$ that has been produced by Huisgen-type copper (I)-catalyzed azide-alkyne cycloaddition (CuAAC) click-chemistry, nanoparticles have been dissolved in DMSO-d$_6$ and we used the same equations described above (Table 3). The percentage of alkyne (% alkyne) that reacted has been evaluated from Eq. (6) where B and T are the respective areas (^{1}H NMR spectra in DMSO-d$_6$) of the PLA methyne protons centered at 5.2 ppm and of the proton of each triazole ring (8.15 ppm). $\overline{DP_n}$ and α are the $\overline{DP_n}$ and the percentage of α-alkyne PLA we used in each formulation, respectively.

$$\%\,\text{alkyne} = \frac{100 \cdot T \cdot \overline{DP_n}}{B \cdot \alpha} \quad (6)$$

2.7. Characterization techniques

^{1}H NMR spectra were recorded on a Bruker Avance 300 apparatus (300.13 MHz, 25 °C) in DMSO-d_6 or $CDCl_3$.

Size exclusion chromatography analyses of dextran derivatives were performed in DMF-LiCl (20 g/L) at 70 °C using a Merck HPLC pump (L-6200A) equipped with a degazer, three PLgel 5 μm columns (10^5 Å, 10^3 Å and 100 Å – Polymer Laboratories). Elution (0.7 ml/min) was dually monitored by multi-angle laser light scattering (MALLS – MiniDawn Tri Star, Wyatt Technology) and differential refractometry (Waters 410). Solutions (10 mg/mL) were prepared by dissolution in the eluent and were left under vigorous stirring for 24 h. Filtration of these solutions was carried out right before injection.

Surface (water/air) tension measurements have been carried out at 25 °C using a K8 surface tensiometer (Krüss, Germany). Surface tensions have been measured using the Wilhemy technique. All samples have been equilibrated for a sufficient time (15 min to 1 h) to reach constant readings.

The size distribution of nanoparticles has been determined in 10^{-4} M NaCl (1 mL of suspension added to 3 mL of NaCl), by dynamic light scattering using a HPPS from Malvern. The mean diameter, D_z (nm), is the so-called *z*-average from cumulant analysis, *i.e.* an intensity-average diameter.

The specific surface area (*Sp*) of the nanoparticles was calculated according to Eq. (7), where ρ is the nanoparticle density calculated by picnometry (here $\rho = 1.26 \times 10^6$ g/m^3).

$$Sp\,(\mathrm{m^2/g\ PLA}) = \frac{6}{\rho D z} \tag{7}$$

From ^{1}H NMR spectrum of washed nanoparticles, one can estimate the amount of dextran per gram of PLA using Eq. (8), where 162 and 72 are the molar masses (g/mol) of glucose unit and of PLA monomer unit, respectively. A_a (4.7 ppm) and B (5.2 ppm) are the areas of anomeric proton and PLA methyne ones, respectively.

$$\mathrm{mg\ dextran/g\ PLA} = \frac{A_\alpha \times 162}{B \times 72} \tag{8}$$

The amount of adsorbed dextran by PLA particle surface unit (Γ in mg/m^2) was calculated using Eq. (9):

$$\Gamma\,(\mathrm{mg/m^2}) = \frac{\mathrm{mg\ dextran/g\ PLA}}{m_{NP} S_p} \tag{9}$$

where m_{NP} is the mass of particles used for analysis.

The electrophoretic mobility of purified nanoparticles has been determined using a Malvern Zetasizer 4 (Mavern Instruments, UK) and studied in NaCl as a function of ionic strength (from 10^{-6} to 10^{-2} M). The zeta potential (ζ) has been calculated from the electrophoretic mobility using the modified Booth equation (Deshiikan & Papadopoulos, 1998). This equation allows the calculation of zeta potential for any k_H and a values, where k_H^{-1} is the Debye length and $D_z/2$ the radius of particles, whereas the classical Smoluchowsky and Hückel equations are applicable only under two limiting cases, $k_H D_z > 100$ and $k_H D_z < 0.1$, respectively. The electrokinetic layer thicknesses (Δ_{PZ}) were calculated from the zeta potential evolution *versus* k_H using the Eversole and Boardman Equation (Eq. (10), Eversole & Boardman, 1941).

$$\ln\left[\tanh\left(\frac{Ze\zeta}{4k_BT}\right)\right] = \ln\left[\tanh\left(\frac{Ze\zeta_0}{4k_BT}\right)\right] - k_H \times \Delta_{PZ} \tag{10}$$

where $z = 1$ (electrolyte valence) and ζ_0 is the surface potential.

The colloidal stability of PLA dispersions toward added electrolyte has been assessed by turbidimetry. Typically, 1 mL of dispersions has been added to 3 mL of NaCl (from 1×10^{-4} to 4 M). The samples have been allowed to stand for 1 h and their absorbance has been measured over the range 450–700 nm, at 50 nm intervals. The slope of the straight line log(optical density) *versus* log(wavelength) was taken as an indication of particle aggregation.

The colloidal stability of suspension toward SDS has been carried out after adding SDS aqueous solution (1% weight) to the suspension. The samples have been allowed to stand for 24 h under stirring. The nanoparticles have been recovered after washing and freeze-drying, then dissolved in DMSO-d_6.

3. Results and discussion

3.1. Azide-multifunctionalized dextran (DexN_3-*n*)

3.1.1. Synthesis of DexN_3-*n*

Azide-multifunctionalized dextrans (DexN_3-*n*) have been synthesized by the reaction described in Scheme 1. Using this reaction and depending on experimental conditions, N_3-end alkyl chains have been linked on dextran leading to various DexN_3-*n* (see supporting info S1). This reaction has been proved as non-degrading reaction for the native dextran (SEC-MALLS experiments, not shown). We found that modification degree (*n*) increased linearly with added amount of compound (1) and the efficiency was evaluated to be equal to 83%. DexN_3-*n* with $n \leq 30\%$ will be used below as water-soluble surfactants. Moreover, if *n* was too high, we observed that hydrophobized dextrans became not well soluble in water, like in case of DexC_6-*n* whose synthesis has already been reported (Rotureau, Chassenieux, Dellacherie, & Durand, 2005; Rouzes et al., 2003).

3.1.2. Adsorption of DexN_3-*n* at air/water interface

Whatever the modification degree of water-soluble DexN_3-*n*, we studied its effect on the steady state surface tension of water that has been measured as a function of the polymer concentration. The results are plotted against the logarithm of the hydrophobic alkyl chains concentration, as shown in Fig. 1. These DexN_3-*n* compounds have been compared to DexC_6-*n* whose surfactant abilities have already been reported (Rouzes et al., 2003). While dextran exhibits no surfactant activity (surface tension equal to 70 nM/m, whatever the aqueous phase concentration), one can see that each DexN_3-*n* and DexC_6-*n* decreases the surface tension of the water phase. It is clear that this lowering is much more pronounced when the modification degree or concentration increases. On other hand, one can see in Fig. 1 that the surface tension lowering is lower in case of DexN_3-*n* compared to DexC_6-*n* for similar *n*. Similar decrease has been observed in case of DexN_3-24 and DexC_6-7 for instance. It could be explained by the presence of N_3 function at the end of each alkyl chain grafted on dextran (DexN_3-*n*). Indeed this function is polar and hydrophilic. Nevertheless, we will observe below that (i) the surface activity of such DexN_3-*n* is sufficient enough to stabilize liquid/liquid interface and (ii) these compounds will provide an hydrophilic shell onto the PLA core of nanoparticles.

3.2. First strategy: nanoprecipitation of dextran-g-PLA

3.2.1. Synthesis of dextran-g-PLA copolymers by click-chemistry

We have already reported on the controlled synthesis of dextran-g-PLA *via* "grafting from" strategy using partially silylated dextran as ring-opening polymerization macroinitiator (Nouvel, Dubois, Dellacherie, & Six, 2004). In this paper, dextran-g-PLA have been obtained using "grafting onto" strategy *via* one click-chemistry step, more precisely the Huisgen-type copper (I)-catalyzed azide-alkyne cycloaddition (CuAAC) (Scheme 1). Since the introduction of this click concept (Rostotev, Green, Fokin, & Sharpless, 2002), various polymer modifications or copolymer syntheses have been reported (Babinot, Renard, & Langlois, 2011; Darcos, El Habnouni, Nottelet, El Ghzaoui, & Coudane, 2010; Le,

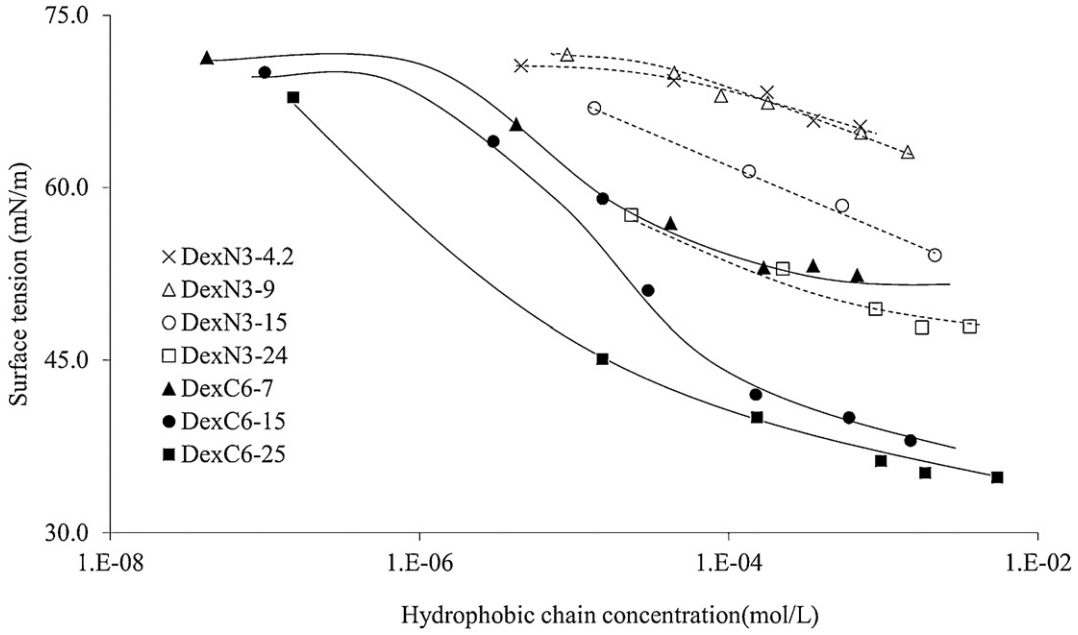

Fig. 1. Surface tension of aqueous $DexN_3$-*n* or $DexC_6$-*n* solutions.

Montembault, Soutif, Rutnakornpituk, & Fontaine, 2010; Nielsen, Wintgens, Amiel, Wimmer, & Larsen, 2010; Tizzotti et al., 2010) and more recently, some reviews deal with copper-free click chemistries (Hoyle & Bowman, 2010; Lowe, Hoyle, & Bowman, 2010; Tasdelen, 2011). CuAAC has been carried out in this paper to prove the studied concept.

Thanks to the Scheme 1 and depending on the experimental conditions, various Dex-g-*x*PLA_m-g-*y*N_3 that exhibit different number (*x*) and length (*m*) of PLA grafts, as well as number (*y*) of residual N_3 functions have been produced (Table 1). Superimposing the Dex-N_3 and purified Dex-g-*x*PLA_m-g-*y*N_3 ^{1}H NMR spectra (see supporting info S2) enables checking the presence of PLA grafted onto the dextran backbone *via* triazole ring. Nevertheless, in this paper, only the copolymers soluble in acetone phase are described. In S3 (supporting info), one can see the SEC curves of initial $DexN_3$ and of α-alkyne PLA, as well as those of pure and unpurified copolymers. As shown, the two copolymer curves are shifted to lower elution volume that means an increase of hydrodynamic volume and certainly of molecular weight (even we know that grafted copolymers and linear chains have not the same behavior in solution). In case of unpurified copolymer, a small shoulder with the same elution volume as α-alkyne PLA chains can be observed, but this shoulder is perfectly removed after precipitation. As shown in Table 1, several copolymers among those synthesized exhibit similar PLA weight fraction (ρ_{PLA} around 80%) but various parameters (*x*, *m*, *y*). From SEC analysis, one can compare the theoretical $\overline{M_n}$ and the value estimated from SEC (SEC $\overline{M_n}$). For each copolymer, *dn*/*dc* has been measured in DMF-LiCl eluent. Taking into account imprecision of SEC measurements, a strong correlation is observed between the two values.

3.2.2. Preparation of dextran-covered nanoparticles

The preparation of dextran-covered nanoparticles by nanoprecipitation has already been reported by us following essentially two strategies. The first one consisted in using PLA dissolved in the organic solvent and a dextran derivative surfactant dissolved in the aqueous phase (Rouzes et al., 2003). During the precipitation, this surfactant adsorbed onto the nanoparticles. An alternative strategy involved the use of dextran-g-polyester copolymers that are oil-soluble (Gavory et al., 2011; Ydens et al., 2005). With those amphiphilic copolymers, another stabilizer has not been required in the aqueous phase. The self-organization of these copolymers allowed the formation of nanoparticles in which polyester chains were essentially in the core while polysaccharide backbone was located in the outer part thus forming a hydrophilic coverage. Multi-cluster aggregates may also be formed.

In this paper, Dex-g-*x*PLA_m-g-*y*N_3 has been dissolved in acetone containing 5% of water (v/v). Actually, previous study (Gavory et al., 2011) proved that acetone is a poor solvent for the Dex-g-PLA, while this is a good solvent for PLA. The addition of a small amount of water (5%) allowed the swelling of dextran backbone and consequently the random coil formation. Indeed water and organic solvent diffuse one to each other during nanoprecipitation. Consequently, a re-arrangement of Dex-g-PLA occurs with dextran backbone swelling, then a contraction driven by the aggregation of PLA grafts leads to the formation of nanoparticles, which have a dextran-enriched surface

3.2.3. Characterization of nanoparticles

In Table 2a are given the mean diameters (D_z) and size distributions (PDI) of the nanoparticles obtained by nanoprecipitation. All the Dex-g-*x*PLA_m used have similar PLA weight fraction (ρ_{PLA} between 75 and 80%). As shown, similar diameters have been obtained but are lower than those of commercial PLA/$DexC_6$-*n* or $DexN_3$-*n* nanoparticles (155 and 150 nm, respectively). This is probably related to the viscosity of the organic phases as shown (Gavory et al., 2011) and as reported in literature (Legrand et al., 2007).

As shown in Table 2a, when Dex-g-*x*PLA_m have been nanoprecipitated, the amount of dextran per gram of PLA was higher than in case of nanoprecipitated commercial PLA in the presence of $DexC_6$-14 surfactant. However, we cannot conclude that dextran is only present in whole of the particle surface. Indeed, during the nanoprecipitation, a part of the dextran may be trapped inside the particle although a dextran-rich surface has been observed as previously established (Gavory et al., 2011).

3.2.4. Colloidal stability in the presence of salt

The colloidal stability of nanoparticles has been examined in water at various NaCl concentrations (ranging from 10^{-4} to 4 mol/L). The stability of nanoparticles in the presence of salt

Table 2
Characteristics of nanoparticles (a) obtained by nanoprecipitation of Dex-g-xPLA$_m$-g-yN$_3$ (10 g/L in organic solvent (acetone/water, 95/5, v/v)) and (b) formulated with o/w emulsion/evaporation technique. α-Alkyne PLA ($\overline{M_n}$ = 8000 g/mol) has been used. The concentration of PLA in organic solvent was 25 g/L.

(a)

Dex-g-xPLA$_m$-g-yN$_3$ *	ρ_{PLA} [a]	D_z (nm)	PDI	mg dextran/g PLA[b]
Dex-g-9.5PLA$_{8000}$	80	125	0.146	-
Dex-g-42PLA$_{1600}$	75	147	0.126	140
Dex-g-82PLA$_{1000}$	75	131	0.085	222

(b)

	DexC$_6$-14 + commercial PLA	DexN$_3$-15 + commercial PLA	DexN$_3$-15 + 50% commercial PLA + 50% α-alkyne PLA + CuBr	DexN$_3$-15 + α-alkyne PLA + CuBr	DexN$_3$-15 + α-alkyne PLA without CuBr
D_z (nm)	120	160	150	150	150
PDI	0.01	0.05	0.10	0.10	0.20
Δ_{PZ} (nm)[c]	11	30		20	
mg dextran/g PLA[b]	216	118	210	382	70
Γ (mg/m^2)[d]	4.45	1.49		6.42	

[a] From Eq. (3).
[b] From Eq. (8). In case of commercial PLA nanoprecipitated in the presence of DexC$_6$-14, the amount of dextran was estimated to be 94 mg dextran/g PLA.
[c] From Eq. (10).
[d] From Eq. (9).

is an important point to consider in view of potential uses like in biological fluids for instance. Furthermore, differences in critical flocculation salt concentration provide a simple means to detect modification in the surface characteristics of nanoparticles according to their conditions of preparation. Above 10^{-3} M NaCl, suspensions of uncoated PLA nanospheres were no more stable, due to the screening of residual surface charges by electrolyte (Gavory et al., 2011). This flocculation originated from Van der Waals attractions which occurred upon increasing ionic strength. This flocculation was shown by a decrease of the straight line slope of log(optical density) *versus* log(wavelength) (d(logOD/$d\lambda$)).

Colloidal stability of the nanoparticles obtained by nanoprecipitation has been studied. On one hand, flocculation was not observed over the whole NaCl concentration range for Dex-g-9.5PLA$_{8000}$ for instance (Fig. 2a). On the other hand, flocculation appeared when increasing NaCl concentration in case of Dex-g-42PLA$_{1600}$, even initial nanoparticles had similar D_z (125 nm *versus* 147 nm). Dex-g-9.5PLA$_{8000}$ and Dex-g-42PLA$_{1600}$ have similar PLA weight fraction but exhibit different number and length of PLA grafts that could explain different chain conformations at the nanoparticles surface and various stabilities. As schematically drawn on S4 (supporting info), copolymers with few long grafts may adopt a "loop" conformation on the nanoparticles surface. These loops become solvated in aqueous medium, thus creating an effective steric barrier that prevents the other particles from approaching too close. This phenomenon is also called entropic stabilization, because when particles approach each other, the solvated loops at particle's surface lose some of their freedom degrees that results in a decrease in entropy. Such entropy decreasing gives rise to repulsive forces, which keep the particles away from each other. In the case of copolymers having many short grafts, chains are certainly more rooted and flattened at the particle surface and do not perfectly conceal the PLA core. In that last case, the colloidal stability of such Dex-g-PLA nanoparticles can be compared to that of particles formulated by nanoprecipitation of commercial PLA with a DexC$_6$-14 or DexN$_3$-15 aqueous phase (Fig. 2a). Whatever the surfactant we used (DexC$_6$-14, DexN$_3$-15 or Dex-g-9.5PLA$_{8000}$) similar stabilities have been observed.

3.3. Second strategy: o/w emulsion/evaporation technique combined with click-chemistry

3.3.1. Emulsification of commercial or α-alkyne PLA with DexN$_3$-n

Nanoparticles have been formulated by an o/w emulsion/evaporation technique that requires energy input during the sonication step. Either commercial PLA or α-alkyne PLA or a 50/50

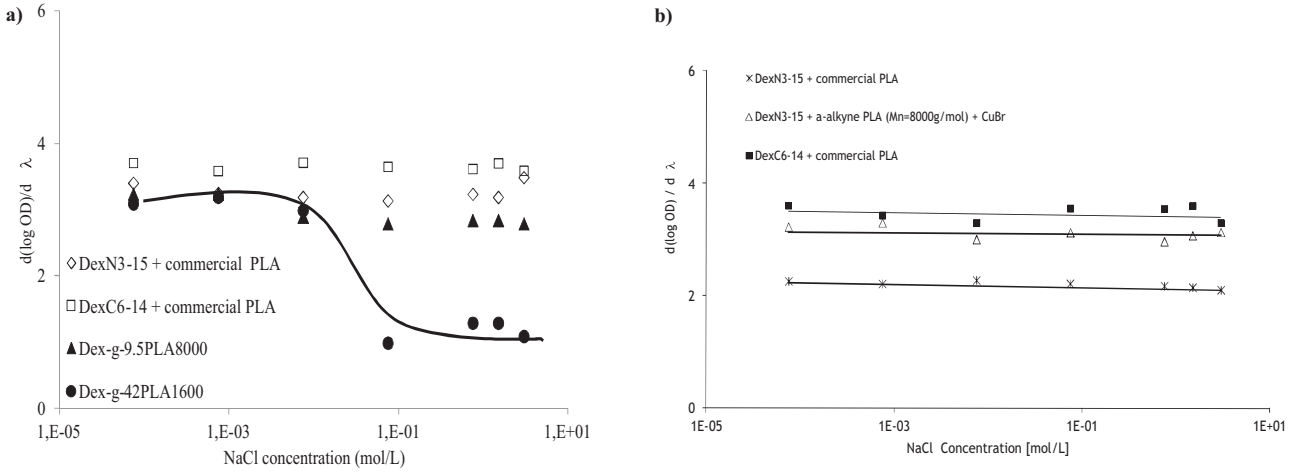

Fig. 2. Colloidal stability of nanoparticles in the presence of NaCl. Case of nanoprecipitation (a). Case of o/w emulsion/evaporation (b).

Table 3
Characteristics of Dex-g-xPLA$_m$-g-yN$_3$ produced at liquid/liquid interface.

	α-Alkyne PLA/commercial PLA weight ratio (%)		
	0	50	100
α-Alkyne PLA (g)[a]	0	0.0125	0.025
Commercial PLA (g)	0.025	0.0125	0
DexN$_3$-15 (g)	0.05	0.05	0.05
N$_3$/alkyne molar ratio	0	26.25	13.12
Dex-g-xPLA$_m$-g-yN$_3$ reduced at the interface	DexN$_3$-15	Dex-g-1.4PLA$_{8000}$-g-13.6N$_3$	Dex-g-2.5PLA$_{8000}$-g-12.5N$_3$
% alkyne[b]	0	36.8	13.1

[a] $\overline{M_n}$ = 8000 g/mol.
[b] Estimated from Eq. (6).

blend of both has been dissolved in the organic phase while DexN$_3$-n (or DexC$_6$-n for comparison) dissolved in the aqueous phase acted as the liquid/liquid stabilizer. Moreover, when CuBr has been added to the emulsion, α-alkyne PLA and DexN$_3$-n reacted together by CuAAC click-chemistry at the liquid/liquid interface. That led to produce amphiphilic Dex-g-xPLA$_m$-g-yN$_3$ chains at this interface, which allowed to covalently link the dextran shell to the nanoparticle's PLA core. Such click-chemistry has been already described during the sonication step (Cintas, Palmisano, & Cravotto, 2011). Nevertheless, some polysaccharide-g-polyester have been already produced at liquid/liquid interface (Colinet, Dulong, Hamaide, Le Cerf, & Picton, 2009) but up to our best knowledge CuAAC click-chemistry has never been carried out at interface to obtain such compounds.

Three experiments have been carried out (Table 3). After nanoparticles purification by repeated washing steps (see Section 2), ^{1}H NMR spectrum in DMSO-d$_6$ has been realized to check if click-chemistry occurred (Fig. 3). As shown, if the nanoparticles have been made in the presence of CuBr, the characteristic peak of the triazole proton appears at 8.15 ppm. In contrast, no peak was observed if the process has been carried out without CuBr or in case of commercial PLA. This proves that the click chemistry has occurred during the sonication step. Nevertheless, the characteristic peaks of PLA and of dextran can be seen on the spectrum of nanoparticles formulated without CuBr (these peaks are of course also shown when CuBr was added). This indicates the physical adsorption of DexN$_3$ at the surface of the nanoparticles made without CuBr (see below). From these spectra, one can evaluate the parameters of such Dex-g-xPLA$_m$-g-yN$_3$ produced at liquid/liquid interface by CuAAC click-chemistry. More precisely, the number of triazole rings *i.e.* the number of PLA grafts (x) and consequently the number of residual N$_3$ (y) could be estimated. We can also calculate the percentage of alkyne functions added in the medium that have been reacted during the sonication step (Eq. (6), Table 3). Whatever this ratio, Dex-g-xPLA$_m$-g-yN$_3$ that have been produced have quite similar parameters. It means that some residual N$_3$ functions could be present at the surface of the nanoparticles and could allow a post-functionalization. Whatever this click-chemistry yield, we will see below that it was enough to ensure a perfectly stable shell that is covalently anchored to the PLA core.

3.3.2. Characteristics of nanoparticles

In Table 2b, one can see that all the nanoparticles formulated by the o/w emulsion/evaporation technique exhibit similar mean diameter (D_z around 150 nm), whatever the PLA and the dextran surfactants used. That proves D_z was not influenced by the presence of α-alkyne PLA. Moreover, carrying out an *in situ* click-chemistry or not, similar D_z have been still observed. When comparing with DexC$_6$-14, we have to mention that nanoparticles produced with DexN$_3$-15 are bigger. This size difference could be due to a larger amount of dextran derivatives on the particle core or to a different adsorption of DexC$_6$ and DexN$_3$. Indeed, alkyl chains of DexC$_6$-14 are more hydrophobic than those present in the DexN$_3$-15 due to the presence of N$_3$ functions at the end-chain. One can also imagine that DexN$_3$-15 has a greater affinity to water, based on the surface tension measurements (Fig. 1). Consequently, DexN$_3$-15 can be proposed to adopt a "loops conformation" on the surface, while a more "tail compact conformation" resulting from stronger interactions between alkyl chain and PLA core can be proposed in case of DexC$_6$-14. Similar results have already been observed when replacing C$_6$ alkyls groups by short PLA grafts (12).

When an *in situ* CuAAC click-chemistry occurred during the sonication step, we observed a clear increase of the dextran amount in the nanoparticles (Table 2b). Indeed, this amount (210, 382 mg of dextran/g of PLA) is twice or three-time the one obtained when DexN$_3$-15 is only physically adsorbed on the commercial PLA nanoparticle surface. Without click reaction, only 118 mg of dextran (70 mg of dextran) per gram of PLA has been estimated when commercial (α-alkyne) PLA has been used with such DexN$_3$. As α-alkyne PLA chains are shorter than those of commercial PLA, DexN$_3$-15 must certainly tangle up with more difficulty in PLA chains in the nanoparticle core. In the same way, when DexC$_6$-14 or DexN$_3$-15 surfactant have been used with commercial PLA, lower dextran amount was observed in case of DexN$_3$-15, in agreement with the lower hydrophobicity of these N$_3$-end alkyl chains. This is not proving that a thicker layer should be obtained when CuAAC click-chemistry takes place *in situ*. But, we believe that the density of the polysaccharidic layer increases with the *in situ* CuAAC click-chemistry (see below).

The electrophoretic mobility of PLA particles covered with DexN$_3$ or DexC$_6$ has been measured in NaCl as a function of the ionic strength. The evolution of zeta potential (ζ) *versus* ionic strength is shown in Fig. 4 for 3 types of nanoparticles that resume all the cases. These particles have been formulated by the o/w emulsion/evaporation technique using commercial PLA or α-alkyne PLA ($\overline{M_n}$ = 8000 g/mol) and DexC$_6$-14 or DexN$_3$-15 as surfactant. In one case, the CuAAC click-chemistry has been occurred during the process. In all curves and whatever the ionic strength, it can be observed that PLA nanoparticles have a negative ζ potential that is attributed to the presence of ionized carboxyl groups on the surface (Colinet et al., 2009). Nevertheless, $|\zeta|$ decreases with increasing NaCl concentration. When comparing nanoparticles made with commercial PLA, one can observe that zeta potential of DexN$_3$-covered nanoparticles exhibits faster neutrality than DexC$_6$-covered ones. When CuAAC click-chemistry has been occurred during the process, similar evolution of zeta potential has been observed and neutrality has been attained at around 3×10^{-3} mol/L of NaCl.

The evaluation of the zeta potential (ζ) allows us to estimate the thickness of the dextran layer (Δ_{PZ}) using Eq. (10). In case of commercial PLA/DexC$_6$-14 nanoparticles, Δ_{PZ} has been evaluated at 11 nm while a 30 nm layer has been observed with DexN$_3$-15 as surfactant, as shown in Table 2b. This three-time thicker shell could be one explanation of the zeta potential neutrality that is

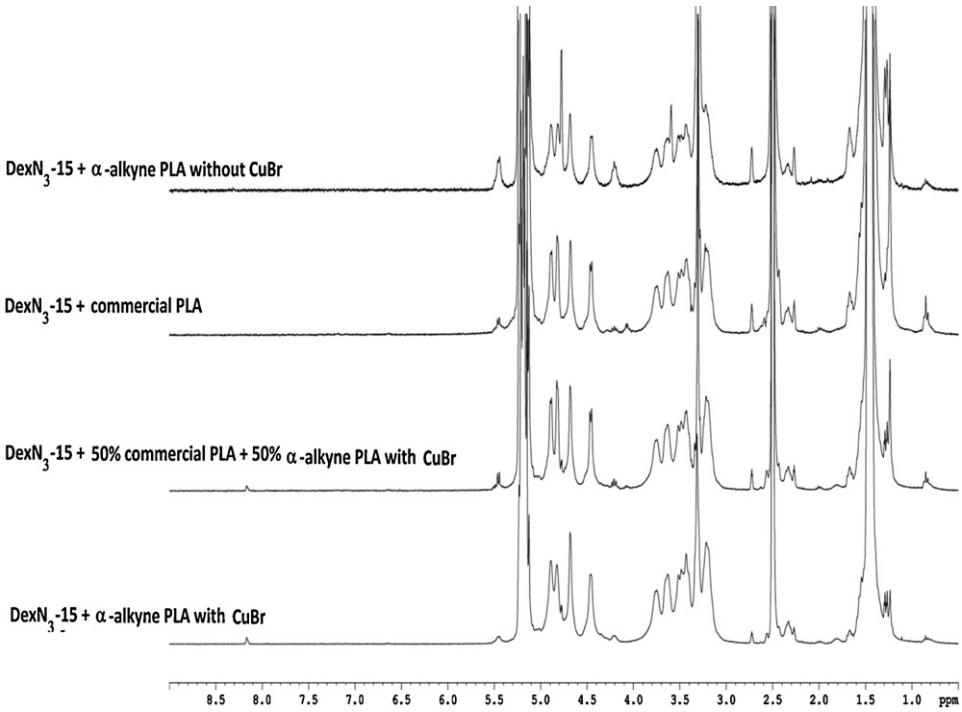

Fig. 3. ^{1}H NMR (DMSO-d_6) spectra of nanoparticles produced *via* o/w emulsion/evaporation technique. DexN_3-15 and various amounts of α-alkyne PLA ($\overline{M_n}$ = 8000 g/mol) have been used with or without addition of CuBr.

faster attained in case of commercial PLA/DexN_3-15 nanoparticles but also of the difference in nanoparticles mean diameter (120 nm *versus* 160 nm). Anyway, it is clear that the dextran shell density (Γ) in case of commercial PLA/DexN_3-15 nanoparticles is lower than using DexC_6-14. This indicates that DexN_3-15, adsorbed at the particle surface, adopts a "loop" conformation in agreement with the polarized character of N_3, while a "tail" conformation may be adopted by DexC_6-14. On the other hand, one can see that in case of *in situ* CuAAC click-chemistry, Δ_{PZ} has been evaluated at 20 nm that is lower than that observed with DexN_3-15. The click-chemistry that occurred at liquid/liquid interface may flatten surfactant chains at the nanoparticle surface that enhances the surfactant anchorage. Consequently, the amount of adsorbed dextran per PLA particle surface unit (Γ) is increasing. Nevertheless, using DexN_3-15 as surfactant (with or without CuAAC click-chemistry) instead of DexC_6-*n* increases Δ_{PZ}.

3.3.3. Colloidal stability in the presence of salt

The colloidal stability of nanoparticles obtained by o/w emulsion/evaporation technique has been studied. Three formulations could be compared as shown in Fig. 2b: commercial PLA has been emulsified with DexC_6-14 or DexN_3-15, while α-alkyne PLA has been reacted with DexN_3-15 during the sonication step. As shown, all these suspensions are quite stable whatever the ionic strength of the water phase. Nanoparticles prepared *via* an *in situ* CuAAC click-chemistry behave similarly to the other ones classically produced.

The CuAAC click chemistry we used during the sonication step (o/w emulsion/evaporation technique) or to previously synthesize

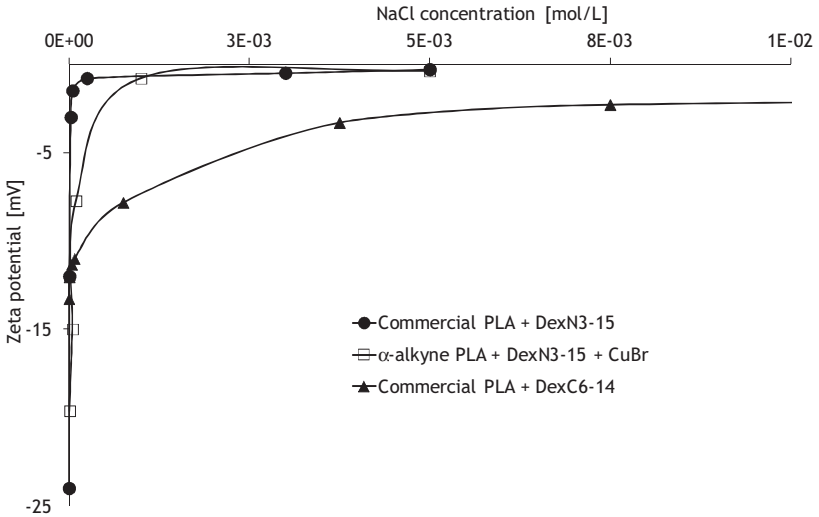

Fig. 4. Zeta potential of nanoparticles made by o/w emulsion/evaporation technique.

Table 4
Amount of dextran (mg dextran/g PLA) in nanoparticles before and after contact with 1 wt% SDS solution.

	$DexC_6$-14 + commercial PLA		$DexN_3$-15 + commercial PLA		$DexN_3$-15 + a-alkyne PLA (8000 g/mol) + CuBr		Dex-g-9.5PLA_{8000}	
	Before SDS	After SDS	Before SDS	After SDS	Before SDS	After SDS	Before SDS	After SDS
o/w emulsion/evaporation	216	0	118	0	382	360	–	–
Nanoprecipitation	94	0	–	–	–	–	210	200

Dex-g-xPLA_m-g-yN_3 (nanoprecipitation) allowed to link in a covalent way the dextran shell to the PLA core, while maintaining size and colloidal stability similar to classical-produced nanoparticles. In the next paragraph, we will verify that these covalent bonds give a strong and permanent anchorage of the shell.

3.4. Colloidal stability of dextran-covered nanoparticles in the presence of SDS

In previous paper (Rouzes et al., 2003), BSA was used as a test protein to evaluate the dextran shell effect on the extent of nonspecific protein adsorption. Dextran shell decreased the interactions of the nanoparticles surface with this protein compared to uncoated PLA particles. This result gave evidence of the effect of the superficial dextran chains steric protection against protein adsorption.

To evaluate the stability of our covalently-linked shell, the colloidal stability of various formulated nanoparticles has been studied in the presence of a drastic anionic surfactant: sodium dodecyl sulfate (SDS). Indeed, desorption of polymeric layers by SDS has already been reported in literature (Blokhus & Djurhuus, 2006; Cattoz, Cosgrove, Crossman, & Prescott, 2012; Lauten, Kjoniksen & Nystrom, 2000; Stolnik et al., 1995). After 1 day contact with 1 wt% SDS solution, nanoparticles have been washed several times, freeze-dried and dissolved in DMSO-d_6 for ^{1}H NMR characterization. Clearly and without doubt, no more peaks characteristic of dextran has been shown on ^{1}H NMR spectra when nanoparticles were produced using $DexC_6$-14 or $DexN_3$-15 (without CuBr) (Table 4, see supporting info S5a). Due to their high affinity for hydrophobic surfaces, molecules of SDS desorbed $DexC_6$-14 or $DexN_3$-15 by competitive adsorption on the PLA surface. This release of dextran-shell proves that here is a physically adsorbed shell to the PLA core. On the other hand, when CuAAC click-chemistry has been carried out previously (nanoprecipitation of Dex-g-xPLA_m-g-yN_3) or *in situ* during the sonication step (o/w emulsion/evaporation), peaks characteristic from dextran (glucosidic protons, anomeric or alcohol ones) are always observed in the ^{1}H NMR spectra. Moreover, no decrease of peaks intensity compared to nanoparticles spectrum before SDS contact has been observed (see supporting info S5b), that means no significant desorption of dextran layer (Table 4). This test confirms that click-chemistry reaction allows fixing in a permanent way the polysaccharide shell to the PLA core. Such nanoparticles should be very stable after their injection into the bloodstream for instance.

4. Conclusions

Dex-N_3 surfactants have been used to produce nanoparticles using two different processes: o/w emulsion/evaporation and nanoprecipitation. As $DexC_6$, these surfactants allow obtaining PLA core/hydrophilic dextran shell nanoparticles with similar characteristics (mean diameter, stability in the presence of salts, ...). Nevertheless, characteristics of the shell (thickness, density, ...) are quite different to those observed with $DexC_6$ surfactants. That is due to the polarized N_3 function at the end of each alkyl chain in $DexN_3$.

The presence of many N_3 functions on dextran chain allows us to carry out a CuAAC click-chemistry before (nanoprecipitation) or during the process (o/w emulsion/evaporation). Nanoparticles with similar characteristics to the previous ones in term of diameter, colloidal stability in presence of salts, ... have been formulated. Nevertheless, higher density of dextran shell covalently-linked to the core has been observed. The permanent hydrophilic shell anchorage has been proved using a drastic anionic surfactant (SDS) that mimic aggressive environment.

A deep characterization of this clicked shell as well as post-functionalization of nanoparticles that exhibit residual N_3 functions will be studied in the next future.

Acknowledgements

Maxime Laville was supported by CNRS and Région Lorraine, while Mélanie Legros by the ANR Particart. The authors express their highest gratitude to Marie-Christine Grassiot for help in SEC measurements and Olivier Fabre for NMR measurements.

Appendix A. Supplementary data

Supplementary data associated with this article can be found, in the online version, at http://dx.doi.org/10.1016/j.carbpol.2012.11.050.

References

Babinot, J., Renard, E., & Langlois, V. (2011). Controlled synthesis of well defined poly(3-hydroxyalkanoate)s-based amphiphilic diblock copolymers using click chemistry. *Macromolecular Chemistry and Physics*, *212*, 278–285.
Bertholon, I., Vauthier, C., & Labarre, D. (2006). Complement activation by core–shell poly(isobutylcyanoacrylate)–polysaccharide nanoparticles: Influences of surface morphology, length, and type of polysaccharide. *Pharmaceutical Research*, *23*, 1313–1323.
Blokhus, A. M., & Djurhuus, K. (2006). Adsorption of poly(styrene sulfonate) of different molecular weights on alpha-alumina: Effect of added sodium dodecyl sulfate. *Journal of Colloid and Interface Science*, *296*, 64–70.
Bravo-OSuna, I., Vauthier, C., Farabollini, A., Palmieri, G. F., & Ponchel, G. (2007). Mucoadhesion mechanism of chitosan and thiolated chitosan–poly(isobutyl cyanoacrylate) core–shell nanoparticles. *Biomaterials*, *28*, 2233–2243.
Carrier, O., Covis, R., Marie, E., & Durand, A. (2011). Inverse emulsions stabilized by a hydrophobically modified polysaccharide. *Carbohydrate Polymers*, *84*, 599–604.
Cattoz, B., Cosgrove, T., Crossman, M., & Prescott, S. W. (2012). Surfactant-mediated desorption of polymer from the nanoparticle interface. *Langmuir*, *28*, 2485–2492.
Cintas, P., Palmisano, G., & Cravotto, G. (2011). Power ultrasound in metal-assisted synthesis: From classical Barbier-like reactions to click chemistry. *Ultrasonics Sonochemistry*, *18*(S1), 836–841.
Colinet, I., Dulong, V., Hamaide, T., Le Cerf, D., & Picton, L. (2009). New amphiphilic modified polysaccharides with original solution behaviour in salt media. *Carbohydrate Polymers*, *75*, 454–462.
Darcos, V., El Habnouni, S., Nottelet, B., El Ghzaoui, A., & Coudane, J. (2010). Well-defined PCL-graft-PDMAEMA prepared by ring-opening polymerisation and click chemistry. *Polymer Chemistry*, *1*, 280–282.
Deshiikan, S. R., & Papadopoulos, K. D. (1998). Modified Booth equation for the calculation of zeta potential. *Colloid and Polymer Science*, *276*, 117–124.
Dupayage, L., Save, M., Dellacherie, E., Nouvel, C., & Six, J. L. (2008). PMMA-grafted dextran glycopolymers by atom transfer radical polymerization. *Journal of Polymer Science Part A: Polymer Chemistry*, *46*, 7606–7620.
Eversole, W. G., & Boardman, W. W. (1941). The effect of electrostatic forces on electrokinetic potentials. *Journal of Chemical Physics*, *9*, 798–801.
Fournier, C., Léonard, M., Le Coq-Léonard, I., & Dellacherie, E. (1995). Coating polystyrene particles by adsorption of hydrophobically-modified dextran. *Langmuir*, *11*, 2344–2347.
Gavory, C., Durand, A., Six, J. L., Nouvel, C., Marie, E., & Léonard, M. (2011). Polysaccharide-covered nanoparticles prepared by nanoprecipitation. *Carbohydrate Polymers*, *84*, 133–140.

Hoyle, C. E., & Bowman, C. N. (2010). Thiol-ene click chemistry. *Angewandte Chemie-International Edition*, *49*, 1540–1573.

Jeong, Y., Na, H. S., Oh, J. S., Choi, K. C., Song, C. E., & Lee, H. C. (2006). Adriamycin release from self-assembling nanospheres of poly(DL-lactide-co-glycolide)-grafted pullulan. *International Journal of Pharmaceutics*, *322*, 154–160.

Jeong, Y. I., Kim, D. H., Chung, C. W., Yoo, J. J., Choi, K. H., Kim, C. H., Ha, S. H., & Kang, D. H. (2012). Self-assembled nanoparticles of hyaluronic acid/poly(DL-lactide-co-glycolide) block copolymer. *Colloids and Surfaces B: Biointerfaces*, *90*, 28–35.

Landoll, L. M. (1982). Nonionic polymer surfactants. *Journal of Polymer Science Part A: Polymer Chemistry*, *20*, 443–455.

Lauten, R. A., Kjoniksen, A. L., & Nystrom, B. (2000). Adsorption and desorption of unmodified and hydrophobically modified ethyl(hydroxyethyl)cellulose on polystyrene latex particles in the presence of ionic surfactants using dynamic light scattering. *Langmuir*, *16*, 4478–4484.

Le, D., Montembault, V., Soutif, J. C., Rutnakornpituk, M., & Fontaine, L. (2010). Synthesis of well-defined omega-oxanorbornenyl poly(ethylene oxide) macromonomers via click chemistry and their ring-opening metathesis polymerization. *Macromolecules*, *43*, 5611–5617.

Legrand, P., Lesieur, S., Bochot, A., Gref, R., Raatjes, W., Barratt, G., & Vauthier, C. (2007). Influence of polymer behaviour in organic solution on the production of polylactide nanoparticles by nanoprecipitation. *International Journal of Pharmaceutics*, *344*, 33–43.

Lemarchand, C., Couvreur, P., Besnard, M., Costantini, D., & Gref, R. (2003). Novel polyester–polysaccharide nanoparticles. *Pharmaceutical Research*, *20*, 1284–1292.

Lemarchand, C., Gref, R., & Couvreur, P. (2004). Polysaccharide-decorated nanoparticules. *European Journal of Pharmaceutics and Biopharmaceutics*, *58*, 327–341.

Lowe, A. B., Hoyle, C. E., & Bowman, C. N. (2010). Thiol-yne click chemistry: A powerful and versatile methodology for materials synthesis. *Journal of Materials Chemistry*, *20*, 4745–4750.

Ma, W. J., Yuan, X. B., Kang, C. S., Su, T., Yuan, X. Y., Pu, P. Y., & Sheng, J. (2008). Evaluation of blood circulation of polysaccharide surface-decorated PLA nanoparticles. *Carbohydrate Polymers*, *72*, 75–81.

Messai, I., Lamalle, D., Munier, S., Verrier, B., Ataman-Onal, Y., & Delair, T. (2005). Poly(D,L-lactic acid) and chitosan complexes: interactions with plasmid DNA. *Colloids and Surfaces A: Physicochemical and Engineering Aspects*, *255*, 65–72.

Nielsen, T. T., Wintgens, V., Amiel, C., Wimmer, R., & Larsen, K. L. (2010). Facile synthesis of beta-cyclodextrin-dextran polymers by "click" chemistry. *Biomacromolecules*, *11*, 1710–1715.

Nouvel, C., Dubois, P., Dellacherie, E., & Six, J. L. (2004). Controlled synthesis of amphiphilic biodegradable polylactide-grafted dextran copolymers. *Journal of Polymer Science Part A: Polymer Chemistry*, *42*, 2577–2588.

Nouvel, C., Raynaud, J., Marie, E., Dellacherie, E., Six, J. L., & Durand, A. (2009). Biodegradable nanoparticles made from polylactide-grafted dextran copolymers. *Journal of Colloid and Interface Science*, *330*, 337–343.

Osterberg, E., Bergstrom, K., Holmberg, K., Schuman, T. P., Riggs, J. A., Burns, N. L., Vanalstine, J. M., & Harris, J. M. (1995). Protein-rejecting ability of surface-bound dextran in end-on and side-on configurations—Comparison to PEG. *Journal of Biomedical Materials Research*, *29*, 741–747.

Ouhib, R., Renault, B., Mouaziz, H., Nouvel, C., Dellacherie, E., & Six, J. L. (2009). Biodegradable amylose-g-PLA glycopolymers from renewable resources. *Carbohydrate Polymers*, *77*, 32–40.

Rostotev, V. V., Green, L. G., Fokin, V. V., & Sharpless, K. B. (2002). A stepwise Huisgen cycloaddition process: Copper(I)-catalyzed regioselective "ligation" of azides and terminal alkynes. *Angewandte Chemie-International Edition*, *41*, 2596–2599.

Rotureau, E., Chassenieux, C., Dellacherie, E., & Durand, A. (2005). Neutral polymeric surfactants derived from dextran: A study of their aqueous solution behavior. *Macromolecular Chemistry and Physics*, *206*, 2038–2046.

Rotureau, E., Léonard, M., Dellacherie, E., & Durand, A. (2004). Amphiphilic derivatives of dextran: Adsorption at air/water and oil/water interfaces. *Journal of Colloid and Interface Science*, *279*, 68–77.

Rouzes, C., Durand, A., Léonard, M., & Dellacherie, E. (2002). Surface activity and emulsification properties of hydrophobically modified dextrans. *Journal of Colloid and Interface Science*, *253*, 217–223.

Rouzes, C., Léonard, M., Durand, A., & Dellacherie, E. (2003). Influence of polymeric surfactants on the properties of drug-loaded PLA nanospheres. *Colloids and Surfaces B: Biointerfaces*, *32*, 125–135.

Stolnik, S., Garnett, M. C., Davies, M. C., Illum, L., Bousta, M., Vert, M., & Davis, S. S. (1995). The colloidal properties of surfactant-free biodegradable nanospheres from poly(β-malic acid-co-benzyl malate)s and poly(lactic acid-co-glycolide). *Colloids and Surfaces A: Physicochemical and Engineering Aspects*, *97*, 235–245.

Tasdelen, M. A. (2011). Diels–Alder "click" reactions: Recent applications in polymer and material science. *Polymer Chemistry*, *2*, 2133–2145.

Tizzotti, M., Labeau, M. P., Hamaide, T., Drockenmuller, E., Charlot, A., & Fleury, E. (2010). Synthesis of thermosensitive guar-based hydrogels with tunable physico-chemical properties by click chemistry. *Journal of Polymer Science Part A: Polymer Chemistry*, *48*, 2733–2742.

Vauthier, C., Persson, B., Lindner, P., & Cabane, B. (2011). Protein adsorption and complement activation for di-block copolymer nanoparticles. *Biomaterials*, *32*, 1646–1656.

Vila, A., Sanchez, A., Tobio, M., Calvo, P., & Alonso, M. J. (2002). Design of biodegradable particles for protein delivery. *Journal of Controlled Release*, *78*, 15–24.

Wang, W., Zhou, S., Sun, L., & Huang, C. (2010). Controlled delivery of paracetamol and protein at different stages from core-shell biodegradable microspheres. *Carbohydrate Polymers*, *79*, 437–444.

Yadav, A. K., Mishra, P., Mishra, A. K., Mishra, P., Jain, S., & Agrawal, G. P. (2007). Development and characterization of hyaluronic acid-anchored PLGA nanoparticulate carriers of doxorubicin. *Nanomedicine*, *3*, 246–257.

Ydens, I., Degée, P., Nouvel, C., Dellacherie, E., Six, J. L., & Dubois, P. (2005). 'Surfactant-free' stable nanoparticles from biodegradable and amphiphilic poly(ε-caprolactone)-grafted dextran copolymers. *e-Polymers*, 046.

Zhang, H., Gao, F., Liu, L., Li, X., Zhou, Z., Yang, X., & Zhang, Q. (2009). Pullulan acetate nanoparticles prepared by solvent diffusion method for epirubicin chemotherapy. *Colloids and Surfaces B: Biointerfaces*, *71*, 19–26.

Zhang, W., Huang, J., Fan, N., Yu, J., Liu, Y., Liu, S., Wang, D., & Li, Y. (2010). Nanomicelle with long-term circulation and enhanced stability of camptothecin based on mPEGylated α,β-poly (L-aspartic acid)–camptothecin conjugate. *Colloids and Surfaces B: Biointerfaces*, *81*, 297–303.

Zille, H., Paquet, J., Henrionnet, C., Scala-Bertola, J., Léonard, M., Six, J. L., Deschamp, F., Netter, P., Verges, J., Gillet, P., & Grossin, L. (2010). Evaluation of intra-articular delivery of hyaluronic acid functionalized biopolymeric nanoparticles in healthy rat knees. *Bio-medical Materials and Engineering*, *20*, 235–242.